nature photonics

PERSPECTIVE

https://doi.org/10.1038/s41566-020-0600-6

Thermophotonic cooling with light-emitting diodes

Toufik Sadi ✉, Ivan Radevici and Jani Oksanen

The currently ubiquitous light-emitting diodes (LEDs) have revolutionized the lighting industry. Contrary to common belief, however, LEDs are much more than just simple electricity-to-light converters. They are solid-state thermodynamic machines, theoretically capable of continuous and near-reversible energy conversion between electrical, thermal and optical energy. For over 50 years, the possibility of exploiting LEDs as efficient solid-state coolers has remained largely out of reach due to the high-material-quality requirements and commercial focus on light emission. Recent promising advances in electroluminescent cooling by LEDs, however, suggest that the remaining challenges in the area may be surmountable and practical cooling could be feasible. This Perspective discusses recent achievements in electroluminescent cooling, outlining the expected promise, the remaining challenges and their potential solutions.

The past few decades have witnessed tremendous progress in developing light-emitting diodes (LEDs) from low-power signal light indicators to the most energy-efficient commercial general lighting technology[1]. Fundamentally, and in contrast to the incandescent light sources, the success of LEDs is largely based on electroluminescence, allowing the dramatic enhancement of the spontaneous emission of radiation at desired parts of the spectrum, without intentionally heating the light source. While the principle of electroluminescence was identified more than a century ago[2], the first LEDs and lasers using gallium arsenide (GaAs) to produce visible light appeared in the 1960s[3]. Since then, extensive research and development work has been carried out to perfect LED technology, with LEDs now dominating multiple signalling, display and lighting applications.

Despite intense research, early identification of the role of thermal energy in electroluminescence[4–7] and the nigh complete understanding of the associated physics, it is still not widely recognized that the currently ubiquitous LEDs are not just simple electricity-to-light converters. Instead, they are solid-state thermodynamic machines that are capable of continuous and near-reversible energy conversion between electrical, thermal and optical energy. In practice, this means that instead of heating up while emitting light, LEDs can actually cool down 'by themselves'. Given that the cooling is based on photon-mediated heat transfer, which may allow efficient operation over a large temperature range, being able to demonstrate the cooling effect has inherent scientific value. Even more importantly, however, it may lead to a currently unexpected cooling and heating technology that provides a more efficient replacement to the widely used thermoelectric coolers (TECs), or even the ubiquitous mechanical heat pumps and refrigerators. Consequently, such solid-state optical refrigerators and heat pumps could be very compact, thin, lightweight, noiseless and vibrationless. They would also not require any hydrofluorocarbon refrigerants and mechanical parts present in compressor-based devices, and they would potentially be able to substantially surpass the largest possible temperature differences reached by thermoelectric devices. As such, they could find use in multiple applications, from on-chip cooling of electronic circuits and sensors to general cooling and heating purposes in the vehicular, domestic and industrial sectors, from near room temperature to close to cryogenic temperatures, all without environmentally harmful refrigerants.

At present, the cooling potential of LEDs is still hidden by the presence of several non-idealities and the partly conflicting industrially driven requirement to maximize the absolute output power of visible LEDs. Nevertheless, the fundamental thermodynamics clearly reveals that optical refrigeration will become possible when the electricity-to-light conversion efficiency of LEDs, generally called the wall-plug efficiency (WPE), exceeds the 100% limit. Reaching this limit will consequently allow a new operating regime for LEDs, enabling completely new functions and applications for optical technologies.

With state-of-the-art LEDs providing efficiencies surpassing 80% (ref. [8]), and the internal and external quantum efficiencies (abbreviated as IQEs and EQEs, respectively) of GaAs materials exceeding 99% (refs. [9–11]), it is justified to ask if, when and how we could more efficiently harness the thermodynamics of light, to develop more sustainable and efficient solid-state heat pump technologies or cryogenic coolers. Recently, this research direction has started to gather more interest among several research groups[12–22], but thoroughly answering this question will require a substantial amount of new insight and technological development, as the deceivingly simple LED encapsulates multiple complex and intertwined features related to physics and technology.

Here we briefly overview the history, fundamental principles and potential of using electroluminescent cooling (ELC) in thermophotonic cooling applications, and address the recent progress and key challenges that need to be considered to harness this potential in practice.

Thermodynamics of electroluminescence

Fundamentally, the possibility of optical refrigeration originates from certain materials' capability to support and maintain an electronic excitation that can enhance the spontaneous emission beyond its thermal value, as described in Box 1. This allows optical energy to flow even against a thermal gradient and, obviously, requires an external source providing energy for the photons. However, as dictated by thermodynamics, a part of the energy of spontaneously emitted light always originates from the thermal energy present in

Engineered Nanosystems Group, School of Science, Aalto University, Aalto, Finland. ✉e-mail: toufik.sadi@aalto.fi

Box 1 | Principles of thermophotonics and efficiency indicators

Principles of thermophotonics. As described by Würfel[36], the spectral irradiance $\mathcal{E}$ of luminescence is given by the product of the photon energy $\hbar\omega$, the optical absorptivity A_b of the object, the optical density of states ρ and the generalized Bose–Einstein distribution F as

$$\mathcal{E}(\hbar\omega, U, T) = \hbar\omega A_b(\hbar\omega) \underbrace{\frac{(\hbar\omega)^2}{4\pi^2\hbar^3c^2}}_{\rho} \underbrace{\frac{1}{\exp[(\hbar\omega - qU)/k_BT] - 1}}_{F((\hbar\omega - qU),T)} \quad (1)$$

where c is the speed of light in the media transporting or generating the light, U is the voltage corresponding to the electronic excitation (that is, the quasi-Fermi level separation between the conduction and valence bands of the excited semiconductor) and T is the emitter temperature. The irradiance $\mathcal{J}$ of the object, including the luminescence above the bandgap (E_g) and the thermal radiation below the gap, is consequently given by

$$\mathcal{J}(U, T, E_g) = \int_{E_g}^{\infty} \underbrace{\mathcal{E}(\hbar\omega, U, T)\mathrm{d}\hbar\omega}_{\text{luminescence}} + \int_{0}^{E_g} \underbrace{\mathcal{E}(\hbar\omega, 0, T)\mathrm{d}\hbar\omega}_{\text{thermal emission}} \quad (2)$$

The essential and only difference to pure thermal radiation in equations (1) and (2) is that the electrical excitation U modifies the emission rate above the bandgap through its contribution to the distribution function F and thereby strongly enhances the spontaneous emission rate of high-energy photons. From the definition of the chemical potential, it further follows that the work needed to create a single photon above the bandgap is equal to qU (and 0 eV below the gap), and the electrical power P per unit surface area needed to drive the light emission of an LED in a lossless thermophotonic system, consisting of the emitter and the (here homogeneous) environment absorbing the radiation, is correspondingly

$$P = (U_b - U_a)J = (U_b - U_a)\int_{E_g}^{\infty} \frac{q}{\hbar\omega} \left[\underbrace{\mathcal{E}(\hbar\omega, U, T)}_{\text{emission}} - \underbrace{\mathcal{E}(\hbar\omega, U_A, T_A)}_{\text{absorption}} \right] \mathrm{d}\hbar\omega \quad (3)$$

where $U_b \geq U$ is the external bias of the LED, $U_a \leq U_A$ and $U_A \leq U$ are, respectively, the external bias of the absorbing environment and the chemical potential of the optical field in the environment, T_A is the ambient temperature and J is the net radiative current density through the LED, consisting of the difference between the emission by the LED and the absorption of photons originating from the environment. The absorption term reciprocally follows the generalized spectral irradiance formula of equation (1), generalizing the description for thermophotonic energy recycling, where the environment also interacts with the emitter and can involve a semiconductor system that harvests energy from the emitted light. Considering the above relations, the conservation of energy further dictates that to emit a photon of energy $\hbar\omega$, it is necessary to also absorb a thermal energy $\hbar\omega - qU$ and the net heat flux (per unit equivalent area) captured by the emitted photons becomes $Q = \mathcal{J}(U, T, E_g) - \mathcal{J}(U_A, T_A, E_g) - U_bJ$. Using the above relations, it is easy to verify that at the monochromatic limit with $A(\hbar\omega) = \delta(\hbar\omega - \hbar\omega_0)$, the COP of the cooling

$$\mathrm{COP} = \frac{Q}{P} \to \frac{\hbar\omega_0 - qU_b}{\hbar\omega_b - qU_a} \xrightarrow{Q\to 0} \mathrm{COP}_{\mathrm{Carnot}} = \frac{T}{T_A - T} \quad (4)$$

approaches the Carnot limit when $Q \to 0$, $(qU - \hbar\omega_0)T_A = (qU_A - \hbar\omega_0)T$ and the electrical biases are equal to the excitations, that is, $U_b = U$ and $U_a = U_A$. At this limit, the processes are also fully reversible and the same considerations apply to energy harvesting.

Efficiency indicators. The efficiency of a thermophotonic system is affected by several physical phenomena as well as the device characteristics. Consequently also, the analysis of the systems typically involves a number of useful figures of merit, most of which are also applied in the analysis of LEDs. The IQE of the LED is the ratio of radiative recombination events to all recombination events, and is typically approximated using the ABC model:

$$\eta_{\mathrm{IQE}} = \frac{Bn^2}{\left(An + Bn^2 + Cn^3 + \sum_s A_s n_s\right)} \quad (5)$$

where A, B and C are the recombination constants for the SRH, radiative and Auger processes, respectively, A_s is the surface/interface recombination coefficient, and n and n_s are the minority carrier densities in the active region and at the surface/interface, respectively. The EQE of the LED is the ratio of extracted photons to injected carriers, and it is related to the IQE by

$$\eta_{\mathrm{EQE}} = \eta_{\mathrm{EXE}}\, \eta_{\mathrm{inj}}\, \eta_{\mathrm{IQE}} \quad (6)$$

where η_{EXE} is the light extraction efficiency and η_{inj} is the injection efficiency (typically ~1 for III–V DHJ structures at practical operating biases). In thermophotonic structures where the light is not extracted to air but collected by a photovoltaic cell, a more meaningful quantum efficiency for the photon transport is the CQE, defined as the ratio of the recovered photocurrent to the current injected to the light emitter[20]. While the various quantum efficiencies determine how large a fraction of the charge carriers or photons is used for their intended purposes, the voltage efficiency η_U of the LED describes how much energy each emitted photon produces, with respect to the electrical energy used to generate it. It can be approximated using the relation

$$\eta_U = \frac{\hbar\omega}{qU_b} = \frac{\hbar\omega}{q(U + RI)} \quad (7)$$

where $\hbar\omega$ is again the photon energy, U_b is the applied external LED bias, U is the internal LED bias corresponding to the effective separation of the quasi-Fermi levels, R is the parasitic series resistance and I is the LED current. The WPE is the electricity-to-light conversion efficiency of an LED and it is given by

$$\eta_{\mathrm{WPE}} = \eta_U\, \eta_{\mathrm{QE}} \quad (8)$$

where η_{QE} is the appropriate quantum efficiency, such as the LED EQE or a thermophotonics device's CQE (or, more accurately, the quantum efficiency for light emission, if available). If the WPE exceeds unity, the LED is able to radiate out more power than it receives from the external power supply, indicating the entrance into the ELC regime. Finally, upon considering the full range of thermophotonic applications, it becomes natural to define the COP for the cooling in accordance with the conventional thermodynamic definitions and the section 'Principles of thermophotonics' above. To eliminate the strong temperature dependence and to compare the performance with the fundamental laws, it is useful to use the SCOP, obtained by dividing the COP by the corresponding Carnot-limited $\mathrm{COP}_{\mathrm{Carnot}}$.

the emitting material. Consequently, light emission can cool down the emitter if the amount of thermal energy extracted by the light exceeds the parasitic heating caused by the non-radiative relaxation processes and other heat-generating non-idealities.

The most mature direct-bandgap semiconductors can be excited externally by both electrical and optical means, allowing optical cooling by electroluminescence and photoluminescence (photoluminescent cooling (PLC)), as illustrated in Fig. 1. In ELC (Fig. 1a, left), the electron–hole pairs entering an LED are provided an energy qU_b by a bias voltage source U_b (q is the elementary charge). On average, they acquire an energy $\hbar\omega - qU_b$ during the thermalization processes they undergo on their way to the active region with a bandgap E_g, mainly determining the average energy $\hbar\omega \geq E_g$ of the emitted photons ($\hbar$ is Planck's constant and ω is the angular photon frequency). For PLC (Fig. 1b, left), in contrast, and as first reported already a century ago[23], the heat capture process is based on a blueshift of a pump laser tuned close to E_g. With sufficiently fast carrier thermalization processes, the spectrum of the re-emitted light is thermally distributed, leading to an average emitted photon energy exceeding that of the absorbed light. The past 25 years have witnessed substantial advances for PLC in doped crystals[24–28]. From the thermodynamics point of view, the only difference between PLC and ELC is the method with which the emitter is excited. This difference nevertheless leads to several different challenges for the two approaches. For example, PLC using III–V semiconductors has thus far been largely barred by the fast decay of excitation efficiency when the pump photon energy falls close to or below E_g (ref. [9]), whereas for ELC, such low-energy excitation does not present a problem. Due to this and the potential benefits PLC provides at very low temperatures, by not necessitating a p–n junction whose performance will be degraded by carrier freeze-out at low temperatures, PLC may hold the greatest promise for cryogenic cooling. However, the topic of PLC has been previously reviewed in literature[27], and hence is not discussed in detail in this Perspective.

In general, all light emission and absorption phenomena — most often considered in partial isolation, for example, in LEDs and photovoltaic devices — should be considered in the framework of thermophotonics that specifically accounts for the inseparable thermodynamic coupling of light emission and absorption. As such, thermophotonics extends and unifies the views conventionally associated only with electroluminescence, photovoltaic energy harvesting or related subdisciplines[29]. Hence, the thermophotonics framework also naturally introduces the idea of combining ELC with the possibility to harvest a part of the emitted photons' energy, leading to the concepts of thermophotonic heat pumps[14] and thermophotonic energy harvesting, as illustrated in Figs. 1c and 1e, right). At the fundamental level, all the optical devices in Fig. 1 can be seen as thermophotonic machines providing access to the optical equivalents of the conventional thermodynamic machines, that is, refrigerators, heat pumps and heat engines. The thermophotonic aspects of the optical energy conversion were initially addressed in the context of enhancing solar energy harvesting[30–32] and optical heat pumps[14]. Later on, the concepts were explored further and extended in several other works, for example, to improve the efficiency of photovoltaic devices[33], to recover waste heat at modestly high temperatures[34] and to consider practical device designs for thermophotonic devices[15,16,35]. Ideally, the processes for cooling and energy harvesting are fully reversible and the same device can switch from acting as a heat pump to converting thermal energy to electricity by simply modifying the device's operating point, when a suitable temperature difference exists. In practice, however, the reversibility may be partly lost by the currently unavoidable losses in the systems and the typically large (several hundreds of kelvin) temperature differences needed to reach reasonable energy-harvesting efficiency. As such, thermal energy generation is expected to have its own set of challenges, which are nevertheless strongly linked to the challenges of ELC in cooling applications. Owing to the differences especially related to the high temperature stability and other modified high-temperature properties of semiconductors, however, the energy-harvesting applications are not specifically addressed in this Perspective.

The promise of thermophotonics

While the efficient operation of thermophotonic energy-harvesting solutions requires high temperatures[30] where present semiconductors are not stable, the thermophotonic heat pump configuration[14] may allow the combination of the best features of several solid-state cooling concepts. Its external properties have substantial similarities to thermoelectric coolers, illustrated in Fig. 1d, while its heat transport mechanism is still based on using photons as the heat carriers. This means that the electrical conductivity between the heat-absorbing photon emitter and the heat-generating photon absorber is not required, eliminating one of the largest obstacles — simultaneously achieving a high Seebeck coefficient and thermal insulation, in part contradicting the Wiedemann–Franz law connecting electrical and thermal conductivities — known to hinder further development of TECs. Finally, recycling the energy available in the emitted photons may allow the efficiency of thermophotonics devices to be boosted to levels that are out of reach for ELC, PLC or TEC alone.

In quantitative terms, the fundamental aspects of light emission by semiconductors are captured in the concepts of the chemical potential of radiation[36] and the accordingly generalized Planck's law (Box 1). This framework also permits the description of the fundamental limiting behaviour of thermophotonic systems, extending from laser refrigeration of solids to electroluminescent coolers and thermophotonic heat pumps. To achieve an initial understanding of various thermophotonic configurations, we compare in Fig. 1 the cooling efficiency of ideal semiconductors at the black-body limit (that is, assuming unity spectral emissivity) by electroluminescent, photoluminescent and thermophotonic systems, as well as a thermoelectric reference system. Figure 1 shows the peak value of the scaled coefficient of performance (SCOP), that is, the ratio of cooling power to electrical power normalized to the Carnot limit, for these coolers, as a function of the temperature and the bandgap energy (or the temperature and the ZT figure of merit for TEC). The SCOPs have been calculated, and scaled by the Carnot COP, for ELC (optimized $U_b = U$, set $U_A = U_a = 0$), PLC (set $U_b = U = E_g$ and $U_A = U_a = 0$) and thermophotonics (optimized both $U_b = U$ and $U_a = U_A$) assuming an ambient temperature $T_A = 300$ K (U_A and U_a are the chemical potential of the optical field in the environment and the external bias of the absorbing environment, respectively). The TEC performance has been evaluated using the model in ref. [37]. For ELC and PLC in the right panels of Fig. 1a,b, the maxima of the SCOPs occur at small bandgaps and only reach roughly 20% and 4% of the Carnot efficiency, respectively. However, small-bandgap materials are not expected to be feasible for cooling due to their low IQEs. In the thermophotonic configuration (Fig. 1c) where the emitted optical energy is recycled by a photovoltaic device, the COPs are dramatically improved, and the relative efficiency is highest for large-bandgap materials, exceeding 60% of the Carnot limit. In theory, the thermophotonics configuration also performs better than TECs in both efficiency and lowest reachable temperatures.

The order of magnitude of the cooling power and costs that can be reached by the optical coolers are equally relevant quantities regarding their practical potential. The order of magnitude of the maximum cooling power achievable by electroluminescence in the black-body approximation with bias voltages approaching the bandgap is shown in the right panel Fig. 1c as a function of the emitter bandgap and temperature. Again, the highest values are reached for large bandgaps and high temperatures, providing cooling powers comparable to 100 W cm^{-2} at bias voltages close to the bandgap. In addition, the values have been calculated assuming optical transport in free space.

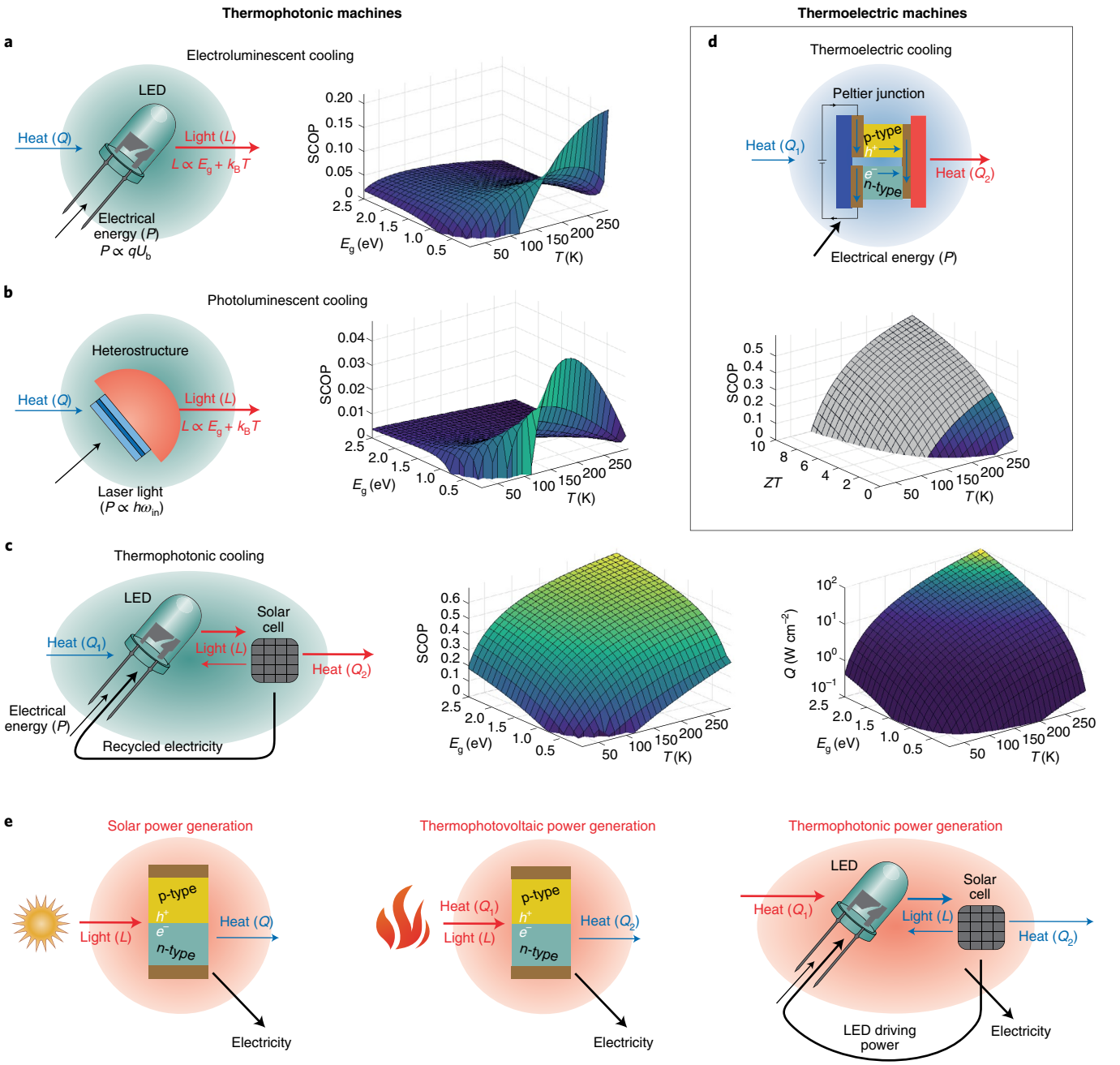

Fig. 1 | Examples of thermophotonic machines for cooling and energy harvesting compared with thermoelectric devices. a–d, The basic principle and potential efficiency of the optical and thermoelectric solid-state coolers. **a**, An LED as an electroluminescent cooler (left) and its predicted Carnot limit SCOP as a function of the active-region bandgap and temperature (right). **b**, An optically pumped semiconductor heterostructure as a photoluminescent cooler (left) and its predicted SCOP (right). **c**, A thermophotonic heat pump combining an LED and a solar cell (left), its predicted SCOP (middle) and maximum achievable cooling power (right). **d**, A typical thermoelectric device (top) and its predicted SCOP as a function of the *ZT* figure of merit and temperature, with the region $ZT > 2$ illustrating the currently hard-to-reach (greyed out) region (bottom). **e**, Examples of thermophotonic engines: a solar cell (left), a thermophotovoltaic device (middle) and an emission-enhanced thermophotonic heat engine (right). In the plots, the ambient temperature is $T_A = 300$ K.

Confining the structure in a semiconductor with a refractive index of that of GaAs ($n_r \approx 3.65$ close to the bandgap[38]), for example, could further increase the cooling power by roughly an order of magnitude due to the dependence of the spectral irradiance (equation (1) in Box 1) on the speed of light in the transporting media. The expected fabrication costs can be estimated by comparing with thin-film solar cells that have been estimated to allow fabrication costs of about US$100 for a 150 cm^2 cell[39]. This would suggest that a cost level in the range US$10–100 for a cell with a cooling capacity of 1 kW could be attainable for possible optical cooling devices in the future if the fabrication process does not involve exceedingly expensive extra steps compared with thin-film solar cell fabrication.

ELC state-of-the-art

The remarkable progress in increasing LED efficiency and output power in the past several decades has been achieved by extensive

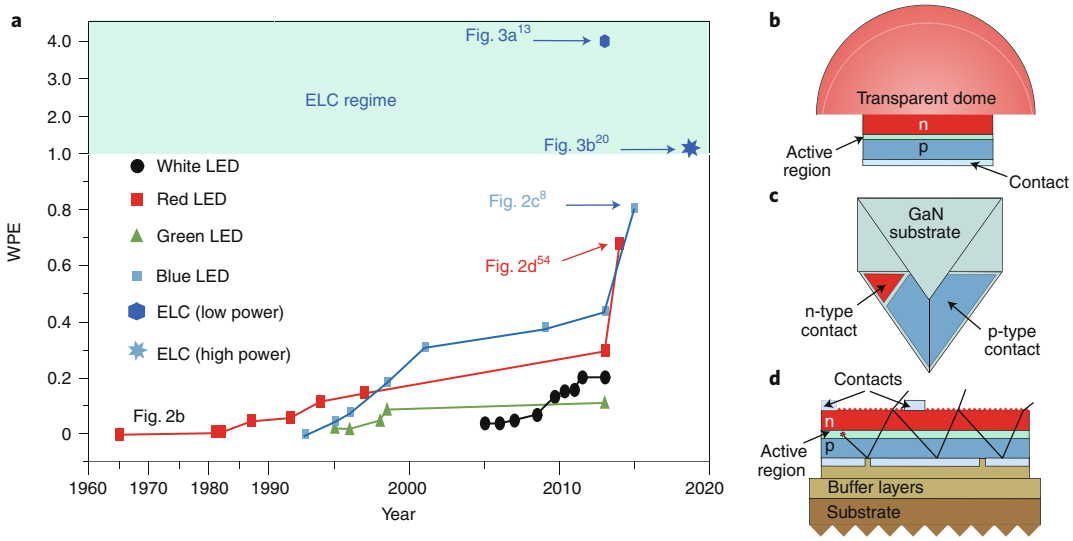

Fig. 2 | Progress of the efficiency of LEDs and selected state-of-the-art LED structures. a, The general evolution of the WPE since the early days of LEDs and links to selected device technologies, indicated by the corresponding figure and reference numbers. ELC data were obtained at room temperature[13,20]. **b**, A DHJ LED using a transparent dome to improve light extraction in early devices. **c**, The flip-chip device with volumetric light extraction. **d**, Thin-film LED with scattering light extraction. The data in **a** are from refs. [8,13,20,54,71]. Panels adapted with permission from: **c**, ref. [8], AIP Publishing; **d**, ref. [54], SPIE.

device engineering, material research and paradigm modifications. This has led to the continuous introduction of new device generations, advances in material engineering and epitaxy, the adoption of the double heterojunction (DHJ) structures, and the development of innovative light extraction methods, gradually improving both quantities by several orders of magnitude. This is particularly well seen in the increase of the WPEs of the LEDs, improving from a fraction of a per cent in the 1960s to the present values close to and even beyond unity, as highlighted in Fig. 2a illustrating the evolution of LED technology and efficiency within the past 60 years.

While the LED industry has recently been mainly focusing on the high-power visible range using GaN, the industrial framework has also fostered a number of attempts to understand and harness the possibilities arising from the thermodynamics and thermophotonic energy transfer in various applications. Initially, the focus of these studies was on the general feasibility of effects related to ELC and thermophotonic heat engines and heat pumps based on semiconductors[14,30–32,40–45]. Later, attention shifted to more concrete devices, ranging from specific thin-film designs to integrated thermophotonic structures[15–17,19]. While most initial computational works focused on conventional large-bandgap III–V semiconductors, for example, GaAs and InP, the first experimental evidence of ELC at extremely small powers was provided by Santhanam et al.[12], using intrinsic GaInAsSb active regions with a bandgap of 0.58 eV. These experiments cleverly maximized the benefits offered by very small bias voltages ($U_b < 100$ μV), allowing extremely small cooling powers ($P_{cool} \approx 50$ pW) even with very small EQEs ($\eta_{EQE} \approx 10^{-4}$) (refs. [12,13]). These demonstrations were subsequently followed by studies on using thermal energy to enhance the efficiency of GaN-based visible LEDs[18] and investigations on the thermophotonic energy transfer processes in GaAs devices[20,46]. Below, we describe in more detail the experimental evidence of ELC put forward by Santhanam et al.[12,13] at very low powers (picowatts), and by us[20] at practical powers using intracavity double diode structures (DDSs).

Ultralow-power setups. Initial demonstrations of ELC by Santhanam et al.[12] showed an unparalleled WPE peaking at about 231% at input powers of the order of tens of picowatts. This very first setup used an LED based on an GaSb/GaInAsSb/GaSb heterostructure with an intrinsic GaInAsSb active region ($E_g \approx 0.58$ eV), where the LED was heated up to temperatures as high as 410 K, increasing the thermal excitation at low forward bias voltages $U_b < k_B T/q$, where k_B is the Boltzmann constant and T is temperature. The emitted light was collected through a collimating lens, as illustrated in Fig. 3a, and measured by a lock-in setup. Subsequently, Santhanam et al.[13] optimized the setup to provide similar results at room temperature. This experiment used an InAs LED emitting at 3.4 μm (~0.366 eV), instead of the 2.15 μm (~0.58 eV) of the original GaInAsSb system. Figure 3c shows the optical output power and the cooling threshold as a function of the input electrical power for their three mid-infrared LEDs, employing active regions made of InAs, InAsSb and InGaAsSb emitting at 3.4, 4.7 and 2.15 μm (~0.366, ~0.264 and ~0.58 eV), respectively. For the first two LEDs with the smallest bandgaps, ELC can be directly observed in the lock-in measurements at room temperature, at very low powers (roughly picowatts), reaching WPEs as high as 400% for the 3.4 μm LED. For the remaining LED, ELC does not manifest itself, potentially due to the less-efficient thermal excitation of the larger-bandgap material at very small bias voltages.

While these extremely small powers are only practical for a limited range of applications[47], they nevertheless provide the first fundamental evidence of ELC, at the extreme low end of the small bias ($qU << E_g/2$) conditions. This also clearly differentiates the small-bias ELC regime from the high-bias regime ($qU \geq E_g/2$) where the output powers can be orders of magnitude larger. The origin of this difference is illustrated in Fig. 3e,f, showing the band diagrams of a GaAs LED for a bias voltage of 0.1 V and 1.3 V, respectively. The amount of thermal energy ~$E_g - qU_b$ needed to create the electron–hole pairs in the active region of the LED is correspondingly ~1.3 eV and ~0.1 eV. Reaching the ELC regime with practically useful LED currents and cooling powers exceeding the A cm^{-2} and mW limits, consequently, will require devices with very high quantum efficiencies and biases close to normal LED operating conditions. Recent experimental[20,46,48,49] and theoretical[19,50] work by us, on intracavity structures, has also brought the first demonstration of ELC at high powers close to reality.

High-power setup. The most successful experimental efforts to demonstrate high-power ELC have thus far focused on the intracavity DDSs studied in refs. [20,46,49] and related simulation works[19,51].

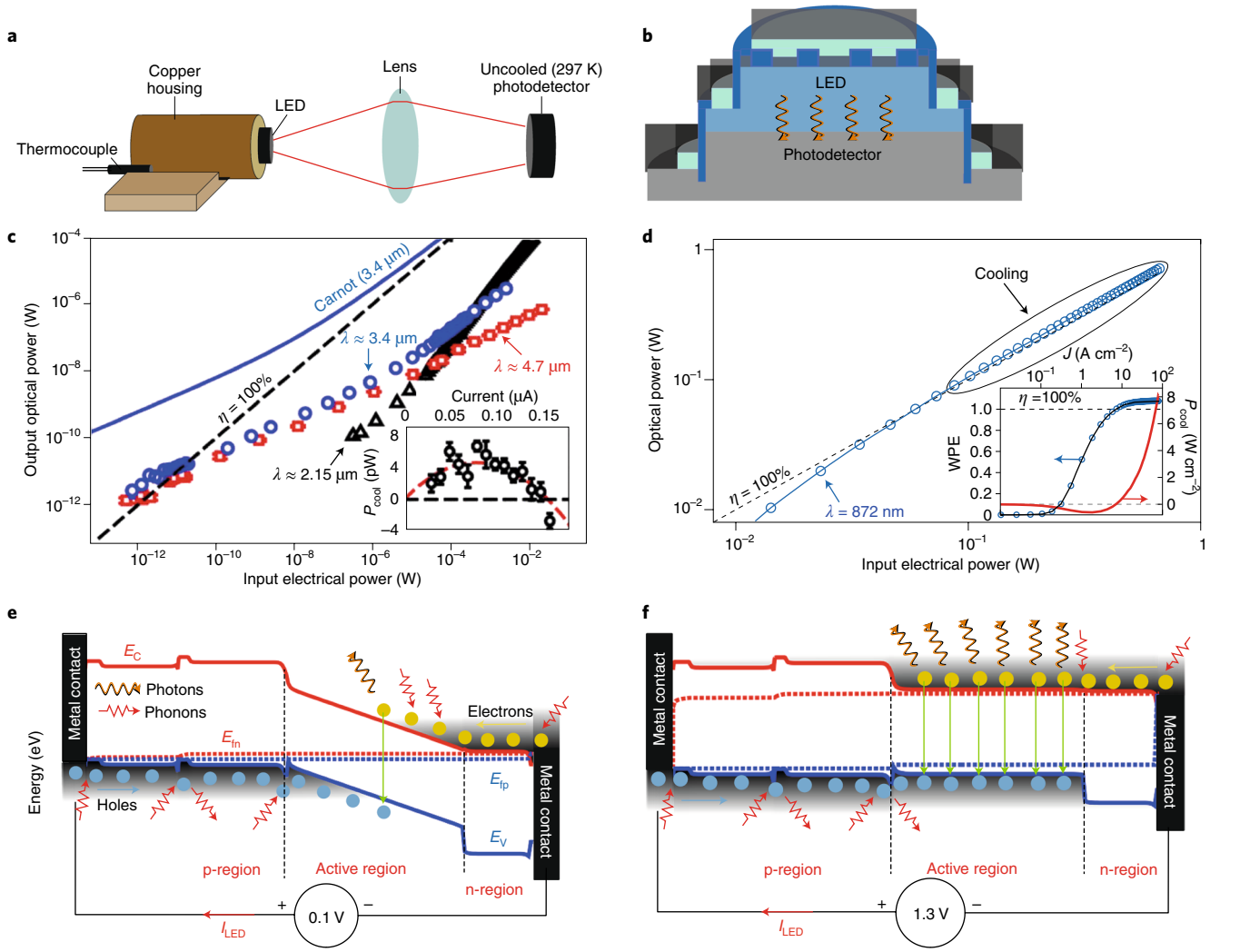

Fig. 3 | Comparison between small- and large-bias ELC. a, The setup used in ref. [13] to measure the over-unity LED efficiencies. **b**, The DDS suggesting internal cooling in ref. [20]. **c**, The optical output power of the small-bandgap LED setup shown in **a**, for the three room-temperature mid-infrared LEDs emitting at wavelengths (λ) of 3.4 μm, 4.7 μm and 2.15 μm as a function of electrical input power, indicating cooling at the very small bias range. The inset shows the cooling power. **d**, The internally generated optical power of the intracavity setup shown in **b**. The inset shows the local WPE and the estimated internal cooling power of the setup. **e**,**f**, A typical band diagram for a GaAs LED structure in ref. [20] at a low 0.1 V bias (**e**) and a high 1.3 V bias close to the bandgap voltage (**f**). *J*, current density; E_C, conduction band edge; E_V, valence band edge; E_{fn} and E_{fp}, quasi-Fermi levels for electrons and holes, respectively. Panels **a** and **c** adapted with permission from ref. [13], AIP Publishing.

The rationale for using the DDS configuration is that it encloses a prototype thermophotonic structure consisting of a GaInP/GaAs DHJ LED and a GaAs p–n homojunction photodetector in a single structure. This eliminates certain substantial light-extraction-related losses encountered in conventional setups, providing a shortcut for studying selected thermophotonic effects at high-current conditions.

A schematic of a DDS is shown in Fig. 3b, enclosing an InGaP/GaAs/InGaP DHJ LED grown on a thick GaAs p–n homojunction photodetector. Light emission from the LED is guided efficiently towards the photodiode, where the absorbed light can be detected by directly measuring the photocurrent of the short-circuited photodetector. Energy transfer efficiency of the DDS is quantified using the coupling quantum efficiency (CQE). In the DDS, heat extraction from the LED is directly demonstrated if the WPE, calculated using the CQE as the effective quantum efficiency (Box 1), exceeds unity. In practice, however, the CQE includes a significant contribution reflecting the photodetector losses, still preventing direct measurement of WPEs exceeding unity[20]. Internal cooling of the LED has nevertheless been indicated when the photodetector losses are accounted for[20]. The prototype DDS uses conventional large-bandgap materials of the AlGaInAsP family, with exceptional bulk qualities[9,52,53]. The best fabricated DDSs exhibit directly measured CQE values as high as ~70–72%, slightly exceeding the highest-reported EQEs of GaAs LEDs[54]. Figure 3d shows the internally generated optical power as a function of the input electrical power, the WPE of the LED obtained by eliminating the contribution of the photodetection and measurement system losses of the current injection probes[20], as well as the corresponding cooling power of the LED in the DDS. This predicts an LED efficiency exceeding unity at the current range 7–80 A cm^{-2}, reaching values up to ~110%, suggesting local LED cooling power densities reaching 8 W cm^{-2}.

ELC challenges and solutions

The discussion above clearly reveals the potential of thermophotonics in cooling applications. In practice, however, reaching the

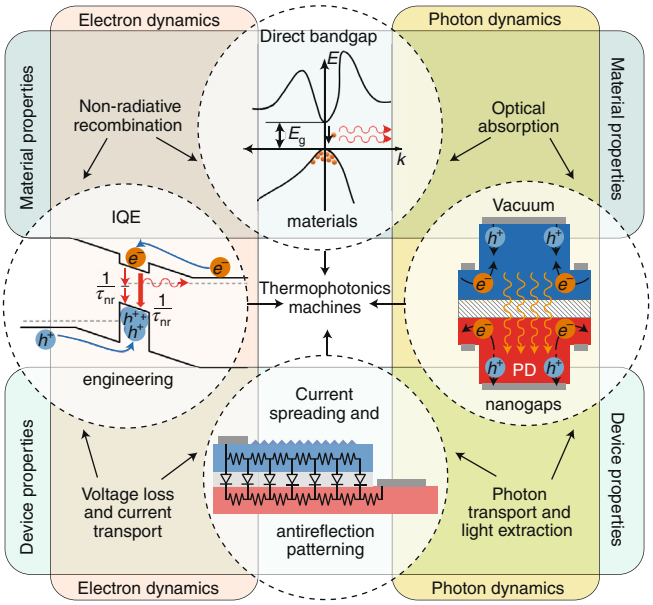

Fig. 4 | Illustration of the key challenges of ELC. In broad terms, the material aspects of the challenges are no longer expected to present a main bottleneck for ELC, while addressing the device-scale challenges will be crucial. PD, photodetector; τ_{nr}, non-radiative recombination lifetime; k, charge carrier wavevector. Left inset adapted with permission from ref. [55], Springer Nature Ltd.

cooling threshold has been challenging, as the eventual WPE of light emission is degraded by several loss mechanisms affecting both the voltage efficiency and the various quantum efficiencies of light emission. While the voltage efficiency can be made to exceed unity even for large resistive losses by simply keeping the bias voltages below the values set by the bandgap, the recombination losses described by various quantum efficiencies, most notably the IQEs and EQEs are less straightforward to optimize. In practice, a suitable combination of η_{QE} and $\eta_U > 1$ (where η_{QE} is the appropriate quantum efficiency and η_U is the voltage efficiency) can nevertheless lead to a WPE exceeding unity, with heat absorption overcoming the internal heat generation. This is the formal condition for observing ELC.

The losses affecting the WPE have multiple origins in phenomena affecting the carrier recombination, light–matter interactions and various transport effects, as illustrated in Fig. 4. The figure further classifies the losses as being related to the electron and the photon dynamics (the vertical columns) as well as to the materials and device design-related challenges (the horizontal rows). This classification illustrates how the electron and photon dynamics couple to the material and device properties, calling for holistic approaches in simultaneously optimizing the recombination, current spreading and optical transport losses towards the threshold, enabling full access to the functionalities provided by thermophotonic machines. In the broader context, we argue that the present bottlenecks for reaching ELC seem to mostly manifest in the device properties row, as discussed below.

The non-radiative recombination losses in an LED originate from the defect-related Shockley–Read–Hall (SRH) recombination as well as the surface, interface and Auger recombination, degrading the IQE as described in equation (5) in Box 1. In general, SRH recombination is a controllable material property that can be made extremely small for GaAs or other high-quality materials, while radiative and Auger recombination are fundamental processes depending mainly on the band structure and also to some extent on the optical or electronic properties of the device. In addition, the recombination statistics generally depend on the carrier densities, enabling also other possibilities to adjust their relative importance by various material and device solutions affecting the carrier densities in the active region. One such approach was recently proposed to extend the range of high-efficiency operation towards smaller input powers by suppressing the relative importance of SRH and interface recombination through active-region engineering, using a GaInP/GaInAs quantum well emitter positioned in the hole-rich region of the p–n junction, enhancing the hole carrier concentrations, and hence the IQE, at input powers relevant for ELC research[55].

The rates of the surface and interface recombination are proportional to the recombination velocity v_s and the effective area of the surface or interface S. The interface recombination velocity for GaAs can generally be made very small by using, for example, GaInP barriers with $v_s \approx 1$ cm s^{-1}. The surface recombination velocity of GaAs, however, can typically approach the thermal velocity $v_{th} \approx 4 \times 10^7$ cm s^{-1}, making surface recombination at device edges a potentially important source of loss[19,20,51]. In practice, surface recombination can be substantially reduced by various surface passivation techniques, including for example, wet passivation techniques typically reducing v_s by at least tenfold[56], epitaxially grown cap layers (for example, III–P)[57] ideally reducing the values down to 1.5 cm s^{-1} (ref. [58]), or controlled oxidation[59] and epitaxial regrowth of III–P layers[57]. Also, reducing the surface area or limiting the transport of carriers to the surface can provide efficient means to suppress surface recombination.

In principle, reaching ELC at large biases ($qU > E_g/2$) requires a high IQE preferably close to unity. This is indeed possible for GaAs, with typical recombination parameters of the order of $A \approx 10^4$–3×10^5 s^{-1} (refs. [9,52,53]), $B = 2 \times 10^{-10}$ cm^3 s^{-1} and $C \approx 10^{-30}$ cm^6 s^{-1} (ref. [60]), generally allowing IQEs exceeding 99% (refs. [9,11]); A, B and C are the recombination constants for the SRH, radiative and Auger processes, respectively. For small-bandgap semiconductors, C is generally large, making high-bias cooling less efficient, if not impossible. The extremely high IQEs dismiss the presence of a fundamental bottleneck for ELC, even if the surface recombination at the device perimeter may introduce additional losses[61] requiring additional engineering.

In the presence of current spreading and voltage losses, the externally applied bias voltage U_b is always larger than the internal (effective) LED voltage $U = U_b - RI$. Consequently, the electrical current spreading resistance R reduces the maximum of the LED current I that can be achieved at above-unity voltage efficiency. Another adverse effect potentially limiting the effective extent of the active region is current crowding[62], which may reduce the attainable power density. Fortunately, both the voltage and current crowding losses can in principle be made quite small by optimizing the contact structures and device geometry[63], although the process itself is subject to several constraints to avoid, for example, increasing the optical losses at the metal contacts or the surface recombination at the LED mesa edges. Some possible geometries that would allow a suitable compromise between electrical and optical losses have been recently suggested and discussed, for example, in refs. [15,16,64]. In addition, new possibilities to optimize the structure could also arise from the back-contacted diffusion-driven structures discussed in ref. [65].

Light confinement due to a large refractive index can severely limit the LED efficiency, constituting one of the largest obstacles for pure ELC. This results from the substantial amplification of the initially small probability of optical absorption at metal contacts and other lossy regions, as well as the non-radiative recombination in the active region following reabsorption. These issues are being addressed, for example, by the various light-management strategies illustrated in Figs. 2b–d and 3b, or other selected schemes relying, for example, on near-field effects[34]. These approaches have allowed GaAs LEDs with a record EQE of 68% (ref. [54]; Fig. 2d), GaN LEDs

with a record EQE of about 80–81% (ref. [8]; Fig. 2c), optically pumped heterostructures with high-refractive-index domes (for example, ZnS or ZnSe) with EQEs of 96% at 300 K (ref. [10]) and 99.5% at 100 K (ref. [9]), and GaAs-based electrically injected LEDs with about 70% and DDS with 72% quantum efficiency, estimated to exhibit internal cooling[20] (Fig. 3b). Renewed efforts of using these efficient light-extraction strategies and the best-available materials in the context of optical cooling could allow conversion of the existing promising results into full optical cooler prototypes.

Future outlook

Considering the advances achieved in optical cooling and the general promises of ELC, it is timely to ask: what will be needed to demonstrate a tangible temperature drop due to ELC at practical LED operating powers? Is it realistic to expect practically useful technologies based on ELC? As the history of LEDs has shown, the loss mechanisms and their interplay make the optimization of the light emission efficiency a complex process, involving multiple disciplines and approaches. This process will not become any simpler when the losses need to be further reduced from the perspective of the full thermodynamic picture. Since the eventual performance of the structures is also expected to be quite sensitive to losses[14,16], developing systems and approaches towards and beyond the cooling threshold is a challenging and resource-intensive task, calling for collective efforts. At present, however, the available experimental results show promising predictions regarding the demonstration of ELC, providing a strong incentive for further research to answer these questions.

Despite the challenges, the present state of the art suggests that the bulk material quality of GaAs is already sufficient for ELC. This implies that the bottlenecks in demonstrating and developing efficient semiconductor ELC systems hinge on designing and fabricating optimal structures, for example, thin-film electroluminescent setups with high-index light extraction lenses. For example, reaching similar quantum efficiencies as in photoluminescent setups[27] would very likely lead to ELC for structures with reasonable resistive losses. This approach would allow a much more favourable voltage efficiency compared with PLC setups, as the driving voltage could be several k_BT/q smaller than the bandgap potential. Also, thermophotonic setups with integrated photon recycling could substantially reduce the light extraction challenges, while necessitating thermal insulation between the light emitter and light absorber. Choosing the most appropriate structure for future works naturally depends on the intended operating biases. While the thermal energy captured by photons has already enabled low-power ELC[13], the requirements for large bias ($U \approx 50$–100% of E_g) ELC are more stringent. In return, the cooling power can become high, ideally exceeding the 10–100 W cm^{-2} range illustrated in the right panel of Fig. 1c.

Considering the fundamentals, it is possible to foresee at least three feasible application areas for ELC: (1) extension or replacement of multistage Peltier coolers, enabling an electrically driven solid-state alternative to reach the higher end of the cryogenic temperature range; (2) new and efficient thermophotonic solid-state cooler/heat pump systems for applications at or close to room temperature; and (3) developing luminaires with above 100% efficiencies. Each application would also have certain special features. (1) Good thermal insulation would be more straightforward to reach, for example, with vacuum-encapsulated thin-film LEDs with domes combining the PLC setups and surface scattering used in the industry[54]. Such non-contact vacuum solutions will allow nearly perfect thermal insulation, but their device area, power and energy recycling capabilities scale less optimally than solutions integrating directly a thermal insulator. (2) DDS- and thermophotonic heat pump-based approaches might be the easiest to demonstrate and are expected to eventually provide the highest cooling power and efficiency. Their performance, however, is likely to depend strongly on the properties of the thermal insulators incorporated within[14], potentially limiting their usefulness to close-to-room-temperature applications. (3) Over-unity efficient LED lighting would most likely be based on GaN materials[18]. This possibility shares obvious synergy with the industrial interests to improve the efficiency of solid-state lighting, and may eventually even lead to unintentionally breaking the 100% limit as a side product of the development.

The development of ELC and thermophotonics has particularly interesting links to GaAs solar cells, thermophotovoltaic systems and photoluminescent cooling, as illustrated in Fig. 1, providing useful concepts for further studies. These include thermal insulation using vacuum nanogaps, highly optimized light extraction methods using ZnS hemispherical lenses and highly optimized materials and epitaxial peel-off solutions. Specifically, and owing to the synergy[66] and recent progress in the III–V (GaAs) and thin-film solar cells, with efficiencies as high as ~29% (ref. [67]) being achieved in single-junction solar cells, knowledge and techniques can be borrowed from solar cell research[68–70] to improve our understanding of ELC. It is also worth remembering that the fundamental predictions in Fig. 1 are based on treating the materials as black bodies. This overlooks any light-management possibilities that might be used to further suppress unwanted thermal emission and to tune the system's spectral properties, allowing substantial further improvements on the fundamental limits of the performance, emissivity and directivity.

In conclusion, recent progress in developing light emitters has provided strong indicators that conventional semiconductors and established fabrication methods have reached a state where the thus far elusive ELC of LEDs is soon becoming feasible. This would lead to a new solid-state cooling method with inherent scientific value. Further development of ELC could also allow the development of cryogenic coolers with an operating range and efficiency far beyond the capabilities of thermoelectric devices. Even more importantly, however, combining ELC with photovoltaic energy recycling could allow the development of thermophotonic heat pumps and coolers with efficiencies and costs that are competitive with those of the ubiquitous compressor-based devices. As the operation of the thermophotonic devices is based on using light as the heat transport agent, they would be fully solid state and require no hydrofluorocarbon-based refrigerants with substantial global warming potential, as is the case for present mechanical devices. As such, optical cooling could eventually make the currently dominating mechanical heat pumps, and their thermoelectric counterparts, obsolete in many applications. While ongoing progress in III–V nanomaterials, LEDs and solar cells is already transforming the corresponding semiconductor energy conversion fields, the future of III–V semiconductor ELC is not void of challenges. However, we believe it also has ample potential to initiate a solid-state cooling revolution that fully parallels the solid-state lighting revolution that has fundamentally disrupted the lighting industry and general lighting in just about one decade.

Received: 25 August 2019; Accepted: 3 February 2020;
Published online: 16 March 2020

References

1. *Solid-State Lighting Research and Development* (US Department of Energy, 2012); http://apps1.eere.energy.gov/buildings/publications/pdfs/ssl/ssl_mypp2012_web.pdf
2. Round, H. J. A note on carborundum. *Electr. World* **49**, 309 (1907).
3. Holonyak, N. & Bevacqua, S. F. Coherent (visible) light emission from $Ga(As_{1-x}P_x)$ junctions. *Appl. Phys. Lett.* **1**, 82–83 (1962).
4. Lehovec, K., Accardo, C. A. & Jamgochian, E. Light emission produced by current injected into a green silicon-carbide crystal. *Phys. Rev.* **89**, 20–25 (1953).
5. Tauc, J. The share of thermal energy taken from the surroundings in the electro-luminescent energy radiated from a p–n junction. *Czech. J. Phys.* **7**, 275–276 (1957).

6. Keyes, R. J. & Quist, T. M. Recombination radiation emitted by gallium arsenide. *Proc. IRE* **50**, 1822–1823 (1962).
7. Dousmanis, G. C., Mueller, C. W., Nelson, H. & Petzinger, K. G. Evidence of refrigerating action by means of photon emission in semiconductor diodes. *Phys. Rev.* **133**, A316–A318 (1964).
8. Hurni, C. A. et al. Bulk GaN flip-chip violet light-emitting diodes with optimized efficiency for high-power operation. *Appl. Phys. Lett.* **106**, 031101 (2015).
9. Bender, D. A., Cederberg, J. G., Wang, C. & Sheik-Bahae, M. Development of high quantum efficiency GaAs/GaInP double heterostructures for laser cooling. *Appl. Phys. Lett.* **102**, 252102 (2013).
10. Gauck, H., Gfroerer, T. H., Renn, M. J., Cornell, E. A. & Bertness, K. A. External radiative quantum efficiency of 96% from a GaAs/GaInP heterostructure. *Appl. Phys. A* **64**, 143–147 (1997).
11. Schnitzer, I., Yablonovitch, E., Caneau, C. & Gmitter, T. J. Ultrahigh spontaneous emission quantum efficiency, 99.7% internally and 72% externally, from AlGaAs/GaAs/AlGaAs double heterostructures. *Appl. Phys. Lett.* **62**, 131–133 (1993).
12. Santhanam, P., Gray, D. J. & Ram, R. J. Thermoelectrically pumped light-emitting diodes operating above unity efficiency. *Phys. Rev. Lett.* **108**, 097403 (2012).
13. Santhanam, P., Huang, D., Ram, R. J., Remennyi, M. A. & Matveev, B. A. Room temperature thermo-electric pumping in mid-infrared light-emitting diodes. *Appl. Phys. Lett.* **103**, 183513 (2013).
14. Oksanen, J. & Tulkki, J. Thermophotonic heat pump — a theoretical model and numerical simulations. *J. Appl. Phys.* **107**, 093106 (2010).
15. Chen, K., Xiao, T. P., Santhanam, P., Yablonovitch, E. & Fan, S. High-performance near-field electroluminescent refrigeration device consisting of a GaAs light emitting diode and a Si photovoltaic cell. *J. Appl. Phys.* **122**, 143104 (2017).
16. Xiao, T. P., Chen, K., Santhanam, P., Fan, S. & Yablonovitch, E. Electroluminescent refrigeration by ultra-efficient GaAs light-emitting diodes. *J. Appl. Phys.* **123**, 173104 (2018).
17. Piprek, J. & Li, Z.-M. Electroluminescent cooling mechanism in InGaN/GaN light-emitting diodes. *Opt. Quantum Electron.* **48**, 472 (2016).
18. Xue, J. et al. Thermally enhanced blue light-emitting diode. *Appl. Phys. Lett.* **107**, 121109 (2015).
19. Sadi, T., Radevici, I., Kivisaari, P. & Oksanen, J. Electroluminescent cooling in III–V intracavity diodes: practical requirements. *IEEE Trans. Electron Devices* **66**, 963–968 (2019).
20. Radevici, I. et al. Thermophotonic cooling in GaAs based light emitters. *Appl. Phys. Lett.* **114**, 051101 (2019).
21. Santhanam, P., Huang, D., Gray, D. J. & Ram, R. J. Electro-luminescent cooling: light emitting diodes above unity efficiency. *Proc. SPIE* **8638**, 863807 (2013).
22. Kuritzky, L. Y., Weisbuch, C. & Speck, J. S. Prospects for 100% wall-plug efficient III-nitride LEDs. *Opt. Express* **26**, 16600–16608 (2018).
23. Pringsheim, P. *Zwei bemerkungen uber den unterchied von luminneszenz- und temperaturstrahlung. Z. Phys.* **57**, 739–746 (1929).
24. Epstein, R. I., Buchwald, M. I., Edwards, B., Gosnell, T. R. & Mungan, C. E. Observations of laser induced fluorescent cooling of a solid. *Nature* **377**, 500–503 (1995).
25. Thiede, J., Distel, J., Greenfield, S. R. & Epstein, R. I. Cooling to 208K by optical refrigeration. *Appl. Phys. Lett.* **86**, 154107 (2005).
26. Sheik-Bahae, M. & Epstein, R. I. Can laser light cool semiconductors? *Phys. Rev. Lett.* **92**, 247403 (2004).
27. Sheik-Bahae, M. & Epstein, R. I. Optical refrigeration. *Nat. Photon.* **1**, 693–699 (2007).
28. Hehlen, M. P. et al. First demonstration of an all-solid-state optical cryocooler. *Light Sci. Appl.* **7**, 15 (2018).
29. Lin, C., Wang, B., Teo, K. H. & Zhang, Z. A coherent description of thermal radiative devices and its application on the near-field negative electroluminescent cooling. *Energy* **147**, 177–186 (2018).
30. Harder, N.-P. & Green, M. A. Thermophotonics. *Semicond. Sci. Technol.* **18**, S270–S278 (2003).
31. Lin, K. L., Catchpole, K. R., Campbell, P. & Green, M. A. High external quantum efficiency from double heterostructure InGaP/GaAs layers as selective emitters for thermophotonic systems. *Semicond. Sci. Technol.* **19**, 1268–1272 (2004).
32. Lin, K. L. et al. Thin semiconducting layers as selective emitters in thermophotonic systems. In *Conference Record of the Twenty-Ninth IEEE Photovoltaic Specialists Conference* 939–942 (IEEE, 2002).
33. Farrell, D. J., Sodabanlu, H., Wang, Y., Sugiyama, M. & Okada, Y. A hot-electron thermophotonic solar cell demonstrated by thermal up-conversion of sub-bandgap photons. *Nat. Commun.* **6**, 8685 (2015).
34. Zhao, B., Santhanam, P., Chen, K., Buddhiraju, S. & Fan, S. Near-field thermophotonic systems for low-grade waste-heat recovery. *Nano Lett.* **18**, 5224–5230 (2018).
35. Zhao, B., Buddhiraju, S., Santhanam, P., Chen, K. & Fan, S. Self-sustaining thermophotonic circuits. *Proc. Natl Acad. Sci. USA* **116**, 11596–11601 (2019).
36. Würfel, P. The chemical potential of radiation. *J. Phys. C* **15**, 3967–3985 (1982).
37. Riffat, S. B. & Ma, X. Improving the coefficient of performance of thermoelectric cooling systems: a review. *Int. J. Energy Res.* **28**, 753–768 (2004).
38. Aspnes, D. E., Kelso, M., Logan, R. A. & Bhat, R. Optical properties of $Al_xGa_{1-x}As$. *J. Appl. Phys.* **60**, 754–767 (1986).
39. Ward, J. S. et al. Techno-economic analysis of three different substrate removal and reuse strategies for III–V solar cells. *Prog. Photovolt.* **24**, 1284–1292 (2016).
40. Catchpole, K. R. et al. High external quantum efficiency of planar semiconductor structures. *Semicond. Sci. Technol.* **19**, 1232–1235 (2004).
41. Min, G. & Rowe, D. M. Conditions for observing the thermo-electro-photo cooling effect. *IET Sci. Meas. Technol.* **1**, 329–332 (2007).
42. Heikkilä, O., Oksanen, J. & Tulkki, J. Ultimate limit and temperature dependency of light-emitting diode efficiency. *J. Appl. Phys.* **105**, 093119 (2009).
43. Malshukov, A. G. & Chao, K. A. Opto-thermionic refrigeration in semiconductor heterostructures. *Phys. Rev. Lett.* **86**, 5570–5573 (2001).
44. Han, P. et al. Analysis of optothermionic refrigeration based on semiconductor heterojunction. *J. Appl. Phys.* **99**, 074504 (2006).
45. Ram, R. J. Thermophotonics for ultra-high efficiency visible LEDs. *Proc. SPIE* **10124**, 1012414 (2017).
46. Olsson, A. et al. Optical energy transfer and loss mechanisms in coupled intracavity light emitters. *IEEE Trans. Electron Devices* **63**, 3567–3573 (2016).
47. Huang, D., Santhanam, P. & Ram, R. J. Low-power communication with a photonic heat pump. *Opt. Express* **22**, A1650–A1658 (2014).
48. Radevici, I., Tiira, J. & Oksanen, J. Lock-in thermography approach for imaging the efficiency of light emitters and optical coolers. *Proc. SPIE* **10121**, 101210Q (2017).
49. Radevici, I., Tiira, J., Sadi, T. & Oksanen, J. Influence of photo-generated carriers on current spreading in double diode structures for electroluminescent cooling. *Semicond. Sci. Technol.* **33**, 05LT01 (2018).
50. Sadi, T. et al. Electroluminescent cooling in intracavity light emitters: modeling and experiments. *Opt. Quantum Electron.* **50**, 18 (2018).
51. Sadi, T., Radevici, I., Kivisaari, P. & Oksanen, J. Electroluminescent cooling in III–V intracavity diodes: efficiency bottlenecks. *IEEE Trans. Electron Devices* **66**, 2651–2656 (2019).
52. Gilliland, G. D., Wolford, D. J., Kuech, T. F., Bradley, J. A. & Hjalmarson, H. P. Minority-carrier recombination kinetics and transport in surface-free GaAs/$Al_xGa_{1-x}As$ double heterostructures. *J. Appl. Phys.* **73**, 8386 (1993).
53. Nelson, R. J. & Sobers, R. G. Minority-carrier lifetimes and internal quantum efficiency of surface free GaAs. *J. Appl. Phys.* **49**, 6103–6108 (1978).
54. Broell, M. et al. New developments on high-efficiency infrared and InGaAlP light-emitting diodes at OSRAM Opto Semiconductors. *Proc. SPIE* **9003**, 90030L (2014).
55. Li, N. et al. Ultra-low-power sub-photon-voltage high-efficiency light-emitting diodes. *Nat. Photon.* **13**, 588–592 (2019).
56. Baca, A. G. & Ashby, C. I. H. *Fabrication of GaAs Devices* (The Institution of Engineering and Technology, 2005).
57. Wada, Y. & Wada, K. GaAs surface passivation by deposition of an ultrathin InP-related layer. *Appl. Phys. Lett.* **63**, 379–381 (1993).
58. Levinshtein, M., Rumyantsev, S. & Shur, M. *Ternary and Quaternary III–V Compounds* (Handbook Series on Semiconductor Parameters, World Scientific Publishing, 1999).
59. Punkkinen, M. P. J. et al. Oxidized In-containing III–V(100) surfaces: formation of crystalline oxide films and semiconductor-oxide interfaces. *Phys. Rev. B* **83**, 195329 (2011).
60. Strauss, U., Rühle, W. W. & Köhler, K. Auger recombination in intrinsic GaAs. *Appl. Phys. Lett.* **62**, 55–57 (1993).
61. Espinet-González, P. et al. Analysis of perimeter recombination in the subcells of GaInP/GaAs/Ge triple-junction solar cells. *Prog. Photovolt.* **23**, 874–882 (2015).
62. Guo, X. & Schubert, E. F. Current crowding and optical saturation effects in GaInN/GaN light-emitting diodes grown on insulating substrates. *Appl. Phys. Lett.* **78**, 3337–3339 (2001).
63. Kuritzky, L. Y. et al. High wall-plug efficiency blue III-nitride LEDs designed for low current density operation. *Opt. Express* **25**, 30696–30707 (2017).
64. Li, Z., Xue, J. & Ram, R. A design of a PhC-enhanced LED for electroluminescence cooling. *Proc. SPIE* **10121**, 1012108 (2017).
65. Myllynen, A., Sadi, T. & Oksanen, J. Diffusion-driven GaInP/GaAs light-emitting diodes enhanced by modulation doping. *Opt. Quantum Electron.* **51**, 90 (2019).
66. Miller, O. D., Yablonovitch, E. & Kurtz, S. R. Strong internal and external luminescence as solar cells approach the Shockley–Queisser limit. *IEEE J. Photovolt.* **2**, 303–311 (2012).
67. Green, M. A. et al. Solar cell efficiency tables (version 54). *Prog. Photovolt.* **27**, 565–575 (2019).

68. Chen, H.-L. et al. A 19.9%-efficient ultrathin solar cell based on a 205-nm-thick GaAs absorber and a silver nanostructured back mirror. *Nat. Energy* **4**, 761–767 (2019).
69. Perl, E. E. et al. Measurements and modeling of III–V solar cells at high temperatures up to 400°C. *IEEE J. Photovolt.* **6**, 1345–1352 (2016).
70. Steiner, M. A. et al. AlGaInP/GaAs tandem solar cells for power conversion at 400°C and high concentration. *AIP Conf. Proc.* **1881**, 040007 (2017).
71. Tsao, J. Y. et al. Toward smart and ultra-efficient solid-state lighting. *Adv. Optical Mater.* **2**, 809–836 (2014).

Acknowledgements

We acknowledge funding from the Academy of Finland, the Photonics Research and Innovation (PREIN) flagship programme and the European Research Council under the Horizon 2020 research and innovation programme (grant agreement number 638173).

We acknowledge the provision of facilities and technical support by Aalto University at the Micronova Nanofabrication Centre.

Competing interests

The authors declare no competing interests.

Additional information

Correspondence should be addressed to T.S.

Reprints and permissions information is available at www.nature.com/reprints.

Publisher's note Springer Nature remains neutral with regard to jurisdictional claims in published maps and institutional affiliations.